Supporting Information

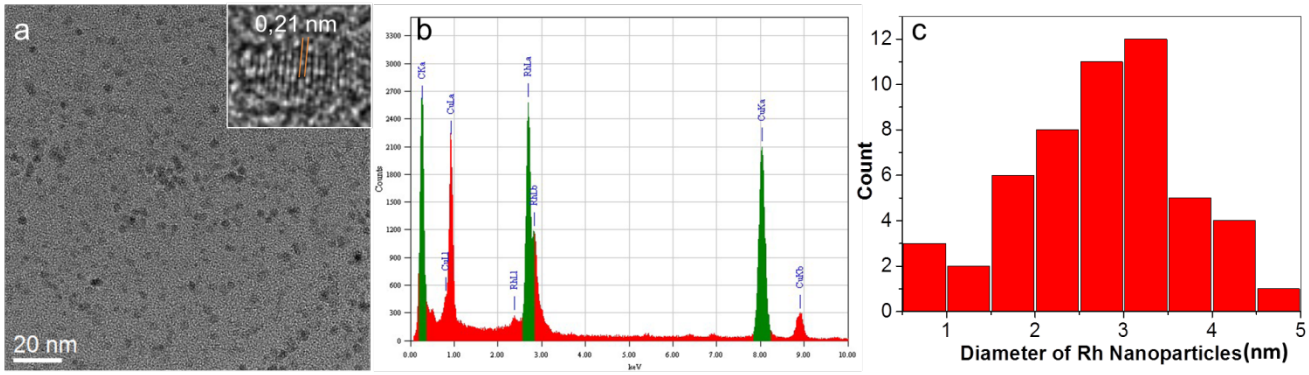

Figure S1. (a) A TEM overview of the Rh nanoparticles prepared through chemical reduction under microwave irradiation. Inset shows a nanoparticle with inter-planar spacing of 0.21 nm, corresponding to the [111] planes of Face-Centered Cubic Rh. (b) Energy-dispersive X-ray microanalysis of Rh nanoparticles. (c) Size distribution of the prepared Rh nanoparticles.

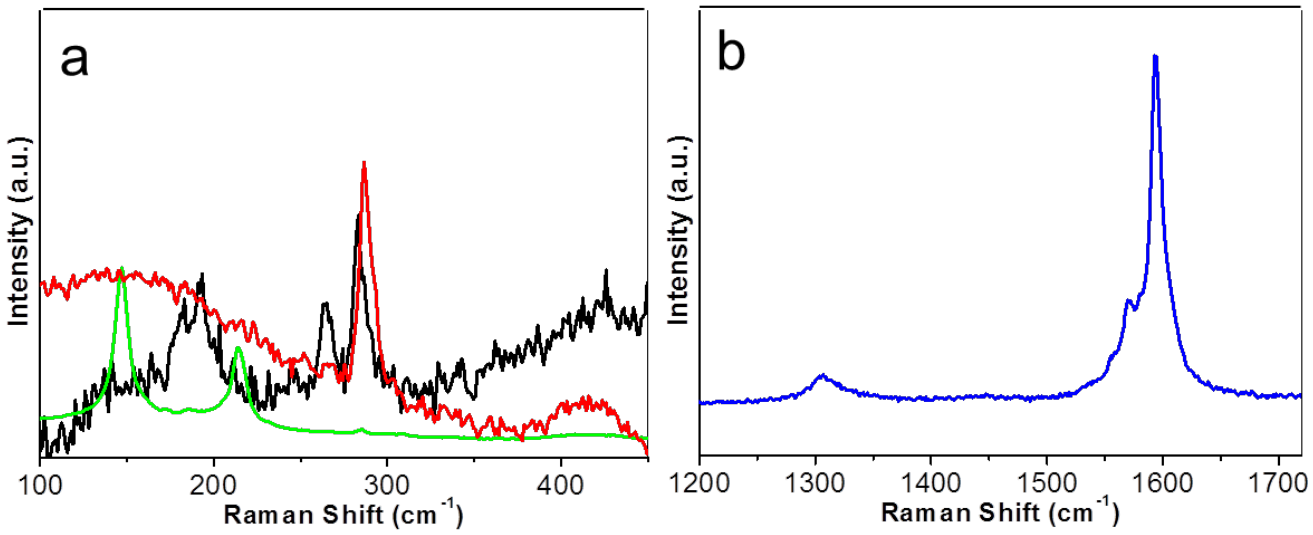

Figure S2. (a) Radial breathing modes of Raman spectra of SWNTs grown on Rh nanoparticles at 800 ^{o}C using CO as the carbon source. (b) A typical high frequency mode showing a relatively high intensity ratio of G to D mode.

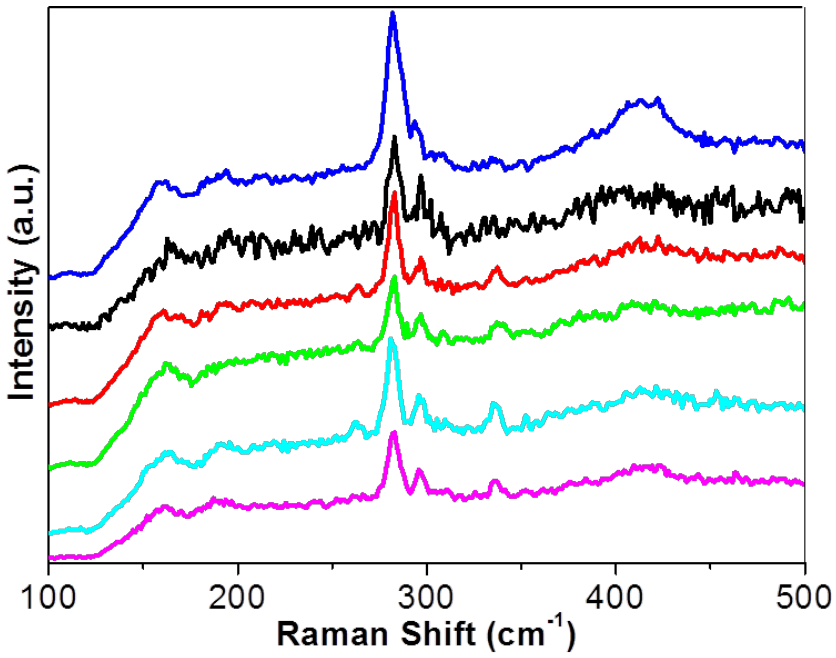

Figure S3. Radial breathing modes of Raman spectra of SWNTs grown on Rh nanoparticles at 700 ^{o}C using CO as the carbon source. The excitation wavelength is 633 nm and the spectra were taken from 6 different points on the sample.

Table S1. (n,m) resolved SWNTs synthesized on Rh catalyst using CO at 800 ^{o}C.

Indices (n,m)	Chiral angle (^{o})	Diameter (nm)	Metallic(M)/Semiconducting(S)
(6,5)	27	0.75	S
(6,5)	27	0.75	S
(6,5)	27	0.75	S
(7,4)	21	0.76	M
(7,4)	21	0.76	M
(6,6)	30	0.81	M
(6,6)	30	0.81	M
(7,5)	24.5	0.82	S
(9,3)	13.9	0.85	M
(8,5)	22.4	0.89	M
(12,0)	0	0.94	M
(8,6)	25.3	0.95	S
(7,7)	30	0.95	M
(11,3)	11.7	1	S
(8,7)	27.8	1.02	S
(8,7)	27.8	1.02	S
(8,7)	27.8	1.02	S
(8,7)	27.8	1.02	S
(9,6)	23.4	1.02	M

(12,2)	7.6	1.03	S
(12,3)	10.9	1.08	M
(9,7)	25.9	1.09	S
(9,7)	25.9	1.09	S
(9,7)	25.9	1.09	S
(9,7)	25.9	1.09	S
(8,8)	30	1.09	M
(11,5)	17.8	1.11	M
(11,5)	17.8	1.11	M
(11,5)	17.8	1.11	M
(14,1)	3.4	1.14	S
(9,8)	28.1	1.15	S
(13,3)	10.2	1.15	S
(10,7)	24.2	1.16	M
(10,7)	24.2	1.16	M
(10,7)	24.2	1.16	M
(11,6)	20.4	1.17	S
(11,6)	20.4	1.17	S
(11,6)	20.4	1.17	S
(9,9)	30	1.22	M
(9,9)	30	1.22	M
(9,9)	30	1.22	M
(9,9)	30	1.22	M
(9,9)	30	1.22	M
(10,8)	26.3	1.22	S
(10,8)	26.3	1.22	S
(10,8)	26.3	1.22	S
(10,8)	26.3	1.22	S
(10,8)	26.3	1.22	S
(10,8)	26.3	1.22	S
(15,1)	3.2	1.22	S
(11,7)	22.7	1.23	S
(11,7)	22.7	1.23	S
(12,6)	19.1	1.24	M
(12,6)	19.1	1.24	M
(12,6)	19.1	1.24	M
(16,0)	0	1.25	S
(10,9)	28.2	1.29	S
(11,8)	24.8	1.29	M
(10,9)	28.2	1.29	S
(12,7)	21.4	1.3	S
(12,7)	21.4	1.3	S
(13,7)	20.2	1.34	M
(10,10)	30	1.36	M
(10,10)	30	1.36	M

(10,10)	30	1.36	M
(11,9)	26.7	1.36	S
(11,9)	26.7	1.36	S
(11,9)	26.7	1.36	S
(11,9)	26.7	1.36	S
(12,9)	25.3	1.43	M
(12,9)	25.3	1.43	M
(11,10)	28.4	1.43	S
(11,10)	28.4	1.43	S
(11,10)	28.4	1.43	S
(11,11)	30	1.49	M
(13,9)	24	1.5	S
(12,10)	27	1.5	S
(14,8)	21.1	1.51	M
(12,11)	28.5	1.56	S
(14,9)	22.8	1.57	S
(14,9)	22.8	1.57	S
(15,8)	20	1.58	S
(12,12)	30	1.63	M
(17,7)	16.5	1.67	S
(13,12)	28.7	1.7	S
(15,10)	23.4	1.71	S
(18,7)	15.7	1.75	S
(14,12)	27.5	1.76	S
(13,13)	30	1.76	M
(13,13)	30	1.76	M
(16,12)	25.3	1.91	S
(18,10)	20.6	1.92	S
(16,13)	26.6	1.97	M
(21,12)	21.1	2.27	M
(21,13)	22.3	2.33	S
(29,23)	26.2	3.54	M
(33,19)	21.2	3.57	S

Table S2. (n,m) resolved SWNTs synthesized on Rh catalyst using methane at 800 ^{o}C.

Indices (n,m)	Chiral angle (^{o})	Diameter (nm)	Metallic(M)/Semiconducting(S)
(10,1)	4.7	0.83	M
(7,7)	30	0.95	M
(8,8)	30	1.09	M
(9,8)	28.1	1.15	M
(9,9)	30	1.22	S
(10,10)	30	1.36	M
(10,10)	30	1.36	M

(10,6)	21.8	1.10	S
(10,7)	24.2	1.16	M
(10,8)	26.3	1.22	S
(10,8)	26.3	1.22	S
(10,8)	26.3	1.22	S
(11,5)	17.8	1.11	M
(11,5)	17.8	1.11	M
(11,7)	22.7	1.23	S
(11,7)	22.7	1.23	S
(11,7)	22.7	1.23	S
(11,7)	22.7	1.23	S
(11,7)	22.7	1.23	S
(11,8)	24.8	1.29	M
(11,8)	24.8	1.29	M
(11,8)	24.8	1.29	M
(11,8)	24.8	1.29	M
(12,11)	28.6	1.56	S
(12,5)	16.6	1.19	S
(12,9)	25.3	1.43	M
(12,9)	25.3	1.43	M
(13,13)	30	1.76	M
(13,2)	7.1	1.11	S
(13,2)	7.1	1.11	S
(13,2)	7.1	1.11	S
(14,8)	21.1	1.51	M
(14,8)	21.1	1.51	M
(15,15)	30	2.04	M
(17,12)	24.3	1.98	S
(17,12)	24.3	1.98	S
(18,18)	30	2.44	M
(20,14)	24.2	2.32	M
(20,17)	27.3	2.51	M
(20,20)	30	2.71	M
(21,15)	24.5	2.45	M
(22,12)	20.4	2.34	S
(22,17)	25.8	2.65	M
(24,13)	20.3	2.55	S
(25,1)	1.9	2.00	M
(25,10)	16.1	2.45	M
(26,9)	14.3	2.47	S
(27,13)	18.6	2.77	S
(28,19)	23.7	3.21	S
(29,17)	21.4	3.16	M
(40,2)	2.4	3.21	S